BJR

Received: 7 May 2015 | Revised: 4 August 2015 | Accepted: 6 August 2015

doi: 10.1259/bjr.20150375

Cite this article as:
Bernsen MR, Guenoun J, van Tiel ST, Krestin GP. Nanoparticles and clinically applicable cell tracking. *Br J Radiol* 2015; **88**: 20150375.

NANOPARTICLES FOR DIAGNOSTIC IMAGING AND RADIOTHERAPY SPECIAL FEATURE: REVIEW ARTICLE

Nanoparticles and clinically applicable cell tracking

[1,2]MONIQUE R BERNSEN, PhD, [1]JAMAL GUENOUN, MD, MSc, [1]SANDRA T VAN TIEL, MSc, and [1]GABRIEL P KRESTIN, MD, PhD

[1]Department of Radiology, Erasmus MC, Rotterdam, Netherlands
[2]Department of Nuclear Medicine, Erasmus MC, Rotterdam, Netherlands

Address correspondence to: Dr Monique R Bernsen
E-mail: *m.bernsen@erasmusmc.nl*

ABSTRACT

In vivo cell tracking has emerged as a much sought after tool for design and monitoring of cell-based treatment strategies. Various techniques are available for pre-clinical animal studies, from which much has been learned and still can be learned. However, there is also a need for clinically translatable techniques. Central to *in vivo* cell imaging is labelling of cells with agents that can give rise to signals *in vivo,* that can be detected and measured non-invasively. The current imaging technology of choice for clinical translation is MRI in combination with labelling of cells with magnetic agents. The main challenge encountered during the cell labelling procedure is to efficiently incorporate the label into the cell, such that the labelled cells can be imaged at high sensitivity for prolonged periods of time, without the labelling process affecting the functionality of the cells. In this respect, nanoparticles offer attractive features since their structure and chemical properties can be modified to facilitate cellular incorporation and because they can carry a high payload of the relevant label into cells. While these technologies have already been applied in clinical trials and have increased the understanding of cell-based therapy mechanism, many challenges are still faced.

INTRODUCTION

Cell-based therapies have, in recent years, been recognized as an important therapeutic option in healthcare.[1] Based on the plasticity and migratory capacity of cells, cell-based therapeutics offer unique possibilities in regenerative medicine, cancer treatment and metabolic diseases.[2–5] For these applications, the ability of cells to repair damaged tissue, act as drug carriers or modulate or enhance natural cellular processes is used as a treatment strategy. Crucial issues for guaranteeing safe and effective use of cell transplants are in determining the most optimal cell type, the route, dose, accuracy and timing of administration, and the persistence and functionality of the transplanted cells. To effectively address these issues, non-invasive visualization of the *in vivo* fate of the transplanted cells may be crucial.[6]

In the past decade, various *in vivo* cell imaging techniques have been developed that enable researchers to track transplanted cells in real-time *in vivo* by optical imaging (OI), MRI single photon emission tomography (SPECT) or positron emission tomography (PET).[7,8] Central to these techniques is the labelling or tagging of the cells prior to transplantation. The most commonly used and the easiest way to achieve this is by introducing a labelling agent into the cells by exposing the cells to the labelling agent in culture.[9–11] The cells then actively incorporate the particles through endocytotic pathways where they generally end up in endosomal compartments.[12] The now cell-associated labelling agent then serves as the signalling beacon by which transplanted cells can be identified in imaging studies (Figure 1). An alternative way of labelling cells is an indirect approach by introducing a reporter gene into the cells of interest. This technology offers various advantages regarding the *in vivo* monitoring of cell fate and function but while widely used in animal models, this approach is currently far from clinical translation and beyond the scope of this review. Interested readers are referred to other reviews dealing with this technology.[13,14]

The main challenge encountered during the cell labelling procedure is to efficiently incorporate the label into the cell, such that the labelled cells can be imaged at high sensitivity for prolonged periods of time, without the labelling process affecting the functionality of the cells. In this respect, nanoparticles offer attractive features since their structure and chemical properties can be modified to facilitate cellular incorporation and because they can carry a high payload of the relevant label into cells.[15]

Figure 1. Nanoparticle labelling and imaging of cells. Top panels: an electron microscopy (left) and fluorescent microscopy (right) image of human umbilical vein cells labelled with iron oxide nanoparticles and fluorescent Gd–liposomes, respectively, showing intracellular presence of the nanoparticles after labelling procedure. Arrows indicate intracellular deposits of iron oxide nanoparticles. Bottom panels: magnetic resonance images obtained from rats injected subcutaneously with cells labelled with iron oxide particles or Gd–liposomes (liposomes containing gadopentetate dimeglumine in the water phase).

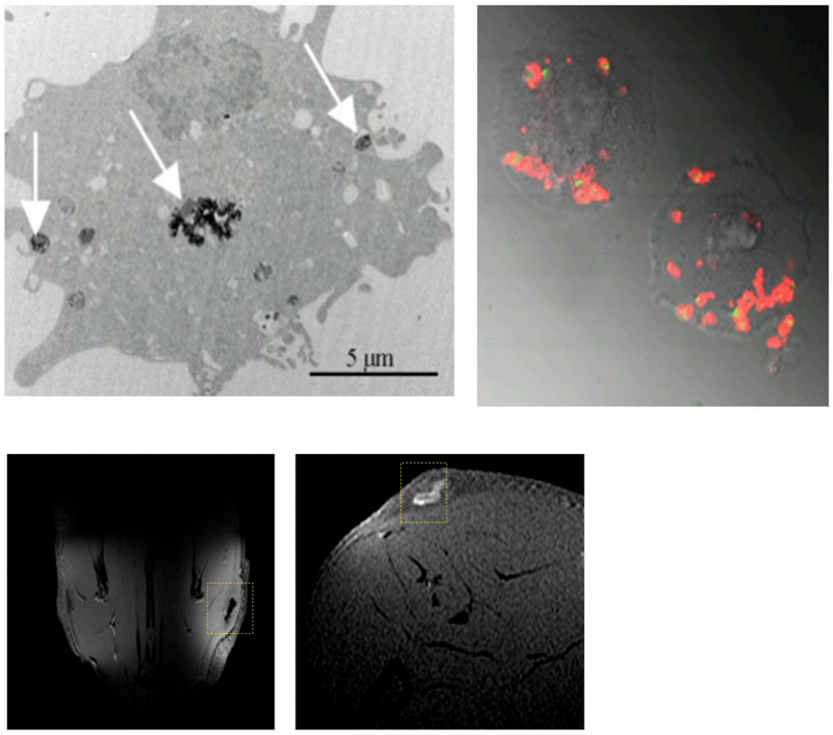

The various imaging techniques each have their own advantages and disadvantages regarding their use in cell tracking studies. OI techniques offer various advantages and have been widely used in pre-clinical studies. The limited tissue penetration capability of light, however, limits the use of these techniques to a large extent to small laboratory animals.[16] Studies aimed at clinical translatability, have therefore focused on MRI, PET or SPECT, which are not limited by signal penetration depths in tissue.[8,17] However, despite the fact that, as of yet, the only FDA-approved cell tracking agent is Indium-111 (^{111}In)-oxine, the use of nuclear imaging techniques for *in vivo* cell tracking beyond lymphocyte scintigraphy, has been limited by concerns regarding radiation damage to cells and the generally short half-life of suitable radioisotopes (in the order of 2 h–6 days). In addition, issues regarding limited intracellular retention of the most commonly used agents are considered an important disadvantage of nuclear imaging approaches for cell tracking.[8,17] Currently, MRI is regarded as the imaging technique of choice for clinically applicable cell tracking. The main advantages of MRI over other techniques are its excellent three-dimensional anatomical imaging capabilities at high resolution together with functional imaging capabilities. The fact that no ionizing radiation is needed makes it therefore suitable for non-invasive and repeatable imaging.

Imaging agents for MRI-based cell tracking can be subdivided into the following categories: superparamagnetic contrast agents (typically containing iron oxide), paramagnetic contrast agents (typically containing gadolinium or manganese), chemical exchange saturation transfer (CEST) agents and non-proton contrast agents (typically containing fluorine). Each of these categories of contrast agents have specific properties with associated advantages and limitations. In many cases, these agents have been used in the form of nanoparticles in order to increase their biocompatibility, delivery efficiency and/or signalling properties. In the following sections, we will discuss the role of the most commonly used nanoparticles and in *in vivo* cell tracking, including recent developments. Some of the key features of these cell labelling agents are summarized in Table 1.

SUPERPARAMAGNETIC IRON OXIDE NANOPARTICLES

Superparamagnetic iron oxide (SPIO) particles typically consist of a crystalline iron oxide (Fe_3O_4 or Fe_2O_3) core coated with a hydrophilic shell of dextran, citrate, polymers or lipids. The iron oxide crystals have a strong magnetic moment, causing a disturbance of the local magnetic field by which they affect the T2 relaxation of surrounding water protons resulting in local signal loss in MR images. After some initial reports in the early nineties, showing the feasibility of tracking iron oxide-labelled cells by MRI,[40,41] many studies followed in which a large variety of iron oxide nanoparticles was studied for their use as cell tracking agents.[42,43] This field of research was especially boosted by the major advances made in stem cell biology and the still increasing interest in cell-based therapies,[1,2] and the realization that *in vivo* cell tracking technology could help in the

Table 1. Most commonly used types of contrast agents (probes) for MRI-based cell tracking

Probe	Basic imaging principle	Main advantage	Main disadvantage	Detection sensitivity (number of cells)[f]	Used for cell tracking in human subjects
Iron oxide nanoparticles	Shortening T2 relaxation of surrounding water protons	High sensitivity	Lack of specific signal; *i.e.* signal loss	1 cell[a,18,19]	Yes[20–29]
Gd-based nanoparticles	Shortening T1 relaxation of surrounding water molecules	Giving rise to signal enhancement	Issues regarding toxicity	300–3000 cells[b,30–32]	No
Manganese-based nanoparticles	Shortening T1 relaxation of surrounding water molecules	Natural body mineral	Issues regarding toxicity	1000–100,000 cells[c,33–35]	No
Chemical exchange saturation transfer agents	Transfer of selectively saturated, exchangeable spins to surrounding bulk water *via* chemical exchange	Multispectral imaging	Requires specialized imaging techniques	10,000 cells[d,36]	No
^{19}F-based nanoparticles	Magnetic spin of ^{19}F nuclei	Not naturally present in body, therefore providing unique signal	Requires specialized imaging techniques	2000–9000 cells[e,37,38]	Yes[39]

^{19}F, fluorine-19.
[a]at intracellular concentrations of 9–50 pg/cell; voxel size 0.26–1 × 10^{-3} mm^3.
[b]at intracellular Gd concentrations of 0.05–70 pg/cell; voxel size 2.24–10.3 × 10^{-3} mm^3.
[c]at intracellular Mn concentrations of 0.35–0.7 pg/cell; voxel size 160 × 10^{-3} mm^3 (only specified by Letourneau et al.[35]).
[d]at intracellular CEST agent concentrations of 3–4 mM/cell; voxel size 24–73 × 10^{-3} mm^3.
[e]at intracellular ^{19}F concentrations of 0.35–0.7 pg/cell; voxel size 660–2000 × 10^{-3} mm^3.
[f]Detection sensitivity is highly dependent of various conditions, such as the cell type, intracellular loading, imaging parameters including voxel size, and magnetic field strength.

development of safe and effective cell-based treatment strategies. Rapid clinical implementation appeared feasible when it was shown that cells could be labelled efficiently with commercially available SPIO particles that were FDA-approved as a liver contrast agent, *i.e.* ferumoxides and ferucarbotran.[44,45] These agents were indeed used in early clinical studies (Table 2), but some practical and technical limitations ultimately prevented more widespread clinical use of SPIO-based cell tracking. Possibly, the first main reason for the limited number of clinical studies with SPIO particles is the fact that manufacturing of the aforementioned preparations was discontinued in the late 90s because of lack of sales for its FDA-approved application for the detection of liver tumours.[21,46] Besides this lack of availability of clinically approved SPIO particles, a number of technical limitations in the use of SPIO particles for cell tracking was also revealed, probably contributing to reduced interest in this technology. The main limitations of SPIO particles are a lack of specificity of the signal,[47] persistence of extracellular deposits[48,49] and very complex quantifiability (Figure 2). Even though in some studies a linear relationship between iron oxide concentration and R2/R2* values[50,51] has been demonstrated, the reliability of such methods is limited since the R2/R2* values are also dependent on intravoxel distribution.[52–54]

However, despite these limitations, SPIO particles are still considered of interest for cell tracking in clinical studies.[21,22,55,56] Main incentives for this continued interest in SPIO particles are the fact that as of yet, they appear to provide the highest detection sensitivity (Table 1), and the vast amount of available data on the safety of the use of SPIO. From the FDA-approved use of ferumoxide and ferucarbotran for liver tumour imaging, systemic safety of SPIO was established. In addition, many studies using these agents for labelling of a variety of cells demonstrated safety of the use of SPIOs for intracellular labelling. In general, no adverse effects on cell survival or cell functionality in terms of differentiation capacity, cytokine release profiles or migratory capacity have been observed. Also in a recently published article in which healthy volunteers were injected with SPIO-labelled peripheral blood mononuclear cells, *in vivo* safety of SPIO cell injections was demonstrated.[25] Therefore, there are continued efforts in generating new, optimized SPIO particles for cell labelling and imaging.[57–59] However, major challenges are faced in going through the regulatory requirements[55,56] and the costs involved may be prohibitive in bringing such particles to the clinic.[56,60] Current strategies seem to be focused on off-label use of already FDA-approved components in generating a SPIO-based intracellular labelling agent.[56,61]

Table 2. Clinical trials with MRI-based cell tracking of magnetic nanoparticle-labelled cells

Study subjects	Cell type	Number of cells and route of administration	Cell labelling agent	Follow-up time with imaging	Main reported finding(s)	Publication year
Patients with melanoma	Autologous dendritic cells	7.5×10^6 cells/ intranodal	Ferumoxide (Endorem; Guerbet)	2 days after transplantation	MRI provided the ability to assess the accuracy of dendritic cell delivery and of internodal and intranodal cell migration patterns	2005[20]
Patients with traumatic brain injury	Autologous neural stem cells	Cell number not specified/intracerebral around the area of brain damage	Ferumoxide[a] (Feridex®; AMAG pharmaceuticals)	24 h and every 7 days for 10 weeks after transplantation	Visualization of neural stem cell proliferation and migration from injection site to perilesional areas based on dynamic signal changes that were similar to patterns of migration observed in a subsequent study performed in rats	2006[28]
Patients with chronic spinal cord injury patients	Autologous bone marrow-derived $CD34^+$ cells	$0.45–1.22 \times 10^6$ cells/ intrathecal into the spinal cord	CD34 monoclonal antibody-coated, micrometre-sized magnetic beads (DynalBeads®; Dynal Biotech)	20 days and 35 days after transplantation	Visualization of hypointense signal areas at the site of injection that redistribute over time suggesting migration of the transplanted cells from the injection site to the lesion site	2007[29]
Patients with Type 1 diabetes	Pancreatic islets	$28–58 \times 10^4$ pancreatic islet equivalents through multiple time-spaced injections/intraportal	Ferucarbotran (Resovist, Schering)	5 days, 6 weeks and 6 months after transplantation	Visualization of transplant-associated hypointense spots in the liver after transplantation that persisted over a period of up to 6 months. Labelling of pancreatic islets did not affect their functionality as evidenced by their retained insulin-producing capacity. Iron overload in the liver as often seen in patients with diabetes interferes with detection of labelled islets	2008[27]
Patients with Type 1 diabetes	Pancreatic islets	$7–68 \times 10^4$ pancreatic islet equivalents/ intraportal	Ferucarbotran (Resovist®, Schering)	1, 4 and 24 weeks after transplantation	Visualization of pancreatic islets grafts in the liver *via* hypointense signal spots. Gradual decrease of the number of hypointense spot over time to 40% of original number. Sensitivity of spot detection was related to the length of labelling time of the pancreatic islets with iron oxide particles. No indications of adverse effects were found	2010[26]
Patients with Multiple sclerosis (MS) and amyotrophic lateral sclerosis (ALS)	Autologous bone marrow-derived mesenchymal stem cells	$60–100 \times 10^6$ cells/ intrathecally and intravenously at a ratio of 2 : 1 of total dose	Ferumoxide[b] (Feridex; AMAG pharmaceuticals)	4 to 48 hours and 1, 3 and 6 months after MSC infusion	MRI indicated possible dissemination of the MSCs from the lumbar site of inoculation to the occipital horns, meninges, spinal roots and spinal cord parenchyma. Observed data support the feasibility for intrathecal injection of cells for treatment of MS and ALS. No cell labelling-associated effects were observed	2010[24]

(Continued)

Table 2. (Continued)

Study subjects	Cell type	Number of cells and route of administration	Cell labelling agent	Follow-up time with imaging	Main reported finding(s)	Publication year
Severe global brain ischaemic injury patient (infant)[e]	Autologous cord blood-derived neural progenitors	12×10^6 cells (25% labelled with iron oxide)/intraventricular in the brain	Ferumoxide[c] (Endorem; Guerbet)	1 day, 1 week, and 1, 2 and 4 months after transplantation.	MRI revealed persistent (4 months) alignment of cell graft (hypointense) along lateral ventricle wall, without evidence of migration into the brain parenchyma. No cell labelling-associated adverse effects were observed.	2010[23]
Healthy volunteers	Peripheral blood mononuclear cells	$1–10 \times 10^8$ cells/ intramuscular or intravenous	Ferumoxide [d](Endorem; Guerbet)	7 days after transplantation	MRI allowed for clear visualization of cell graft. Cell dose-dependent reduction of signal intensity in liver and spleen following intravenous cell injection, indicating dose-dependent accumulation of injected cells in these organs. Migration of labelled cells to an induced site of inflammation (performed in one volunteer). No cell labelling-associated adverse effects were observed.	2012[25]
Patients with Type 1 diabetes	Pancreatic islets	32×10^4 pancreatic islet equivalents/ intraportal	Ferucarbotran (Resovist, Schering)	6 months after transplantation	Feasibility of using positive MRI techniques of iron oxide-labelled cells in a clinical setting with potentially improved transplanted cell identification capabilities.	2014[21]
Severe global brain ischaemic injury patient (infant)[e]	Autologous cord blood-derived neural progenitors	12×10^6 cells (25% labelled with iron oxide)/intraventricular	Ferumoxide[c](Endorem; Guerbet)	1 day, 1 week, and 1, 2, 4, 33 months after transplantation.	Total dissipation of the labelled cell-associated hypointense spots over prolonged period of time. Demonstrated *in vitro* feasibility of forced migration of iron-labelled cells by an external magnet.	2014[22]
Patients with colorectal adenocarcinoma	Autologous dendritic cells	$1–10 \times 10^6$ cells/ intradermal	Clinical grade perfluorocarbon nanoparticles (CS-1000, Celsense, Inc)	4 and 24 h after transplantation	Visualization of cell graft at site of injection at 4 h post transplantation with a approximately 50% reduction of signal at 24 h using a scan time of 10 minutes. No imaging evidence of migration of labelled cells was found possibly due to limited detection sensitivity. No cell labelling-associated adverse effects were observed	2014[39]

Endoorem, Guerbet, Sulzbach, Germany; Feridex, AMAG Pharmaceuticals, Cambridge, WA; Dynal beads, Dynal Biotech, Osio, Norway; Resovist, Schering, Berlin, Germany; CS-1000, Celsense Inc., Pittsburgh, PA.
[a]A non-clinical grade transfection agent (Effectene®; Qiagen, Hilden, Germany) was used to promote cellular uptake of the iron oxide nanoparticles.
[b]The transfection agent poly-L-lysine was used to promote cellular uptake of the iron oxide nanoparticles.
[c]The transfection agent poly-L-lysine (Sigma, St Louis, MI) was used to promote cellular uptake of the iron oxide nanoparticles.
[d]Clinical grade protamine sulphate was used as a transfection agent to promote cellular uptake of the iron oxide nanoparticles.
[e]The studies by Jozwiak et al[23] from 2012 and Janowski et al[22] from 2014 report on the same patient, with the article by Janowski reporting on longer follow-up of this patient and additional *in vitro* experiments on the labelled cells.

PARAMAGNETIC GADOLINIUM-BASED NANOPARTICLES

Gadolinium(III) chelates are the most commonly used contrast agents in clinical MRI and are generally characterized as T1 or positive contrast agents. The seven unpaired electrons of the Gd^{3+} ion create a magnetic moment that accelerate the relaxation of surrounding water protons typically resulting in signal enhancement on MR images. The possibility of obtaining positive contrast from labelled cells instead of negative contrast as obtained with SPIOs has been considered a major advantage and stimulated the use of Gd-based nanoparticles for cell labelling. Particulate Gd contrast agents were shown to be far more effective than regular Gd chelates in terms of the amount of Gd initially incorporated and the retention of Gd in the cell over time.[31,62,63] Various particulate formulations of Gd-based cell tracking agents have been developed over the past few years including liposomal[31,64] and micellar[63,65] nanoparticles, polymer-coated Gd–oxide particles[32,66,67] and carbon nanostructures[68] in order to increase cellular loading with Gd or to increase the signalling capacity by increasing the T1 relaxivity.

A remarkable finding with Gd-based cell labelling has been that Gd-labelled cells showed different contrast behaviour depending on the labelling strategy used and/or the specific environmental circumstances. In contrast to an expected signal enhancement, clusters of Gd-labelled cells were found to give rise to signal loss under both *in vivo* and *in vitro* conditions.[31,69,70] Explanations for this phenomenon include aspects regarding the local concentration of Gadolinium and the effect of compartmentalization of the Gd-based agents influencing the rate of exchange and the availability of free water protons. Capitalizing on the compartmentalization effect, Guenoun et al[71] proposed using the changing contrast behaviour of cells labelled with gadolinium liposomes as a read out method for assessing the functional status of injected cells (Figure 3). They showed that at an identical Gd concentration, Gd incorporated inside the cell gave rise to signal loss while Gd released from non-viable cells resulted in signal gain which quickly dissipated.[31,71]

Despite the fact that various studies showed limited or no adverse effects of the Gd-based labelling agents on the functionality of labelled cells at relevant labelling concentrations,[31,62,63,66,68,72] major concerns regarding the toxicity of the long-term presence of ionic Gd exist,[70,73,74] which may limit introduction of such agents into the clinic. Gadolinium contrast agents have been associated with the occurrence of nefrogenic systemic fibrosis in patients with impaired kidney functions, and Modo et al[74] reported on a negative effect on disease pathology of implanted neural stem cells labelled with the Gd-based contrast agent GRID (Gadolinium-Rhodamine Dextran) in a rat stroke model.

PARAMAGNETIC MANGANESE-BASED NANOPARTICLES

Similar to Gd, manganese is also known as a T1 contrast agent, shortening the relaxation time of surrounding water protons. Because of the concerns regarding the cellular toxicity of Gd ions, manganese has been studied as an alternative positive contrast agent for cell labelling. Manganese is a natural cellular component and functions, for instance, as a cofactor for enzymes and receptors. Manganese as a contrast agent has been used in the form of manganese chloride (FDA-approved). Initial studies on the use of manganese-based agents for cell labelling and imaging also used $MnCl_2$.[75] Moreover, because of the fact that manganese is transported by calcium channels, $MnCl_2$ has been proposed as a cell labelling agent by which a direct read out of the viability of cells would be possible.[76] Because of the low relaxivity properties of $MnCl_2$, nanoparticle formulations of manganese have been explored as T1 agents for cell labelling. This involves manganese oxide particles with variations in coating with the goal to improve biocompatibility, stability and/or relaxivity.[34,35,77] Most recently silica-coated MnO particles were shown to have excellent relaxivity properties, also at magnetic field strengths >3.0 T. This allowed for highly sensitive, positive contrast detection of MnO-labelled cells; in the order of several thousand cells (Table 1). Unfortunately, however, in various reports significant effects of MnO particles on cell functionality have also been reported, such as reduced cell survival[33,76,78] and impaired multipotent differentiation capacity.[34,79] These findings may significantly reduce interest for clinical translation of such approaches.

CHEMICAL EXCHANGE SATURATION TRANSFER - AGENT NANOPARTICLES

CEST agents are a special class of contrast agents for MRI. CEST agents contain slow exchangeable protons that can be selectively saturated by an off-resonance pulse upon which the saturation is transferred to surrounding bulk water *via* chemical exchange.[80] The possibility to generate multiple contrast signatures by choosing agents with unique and different resonance frequencies, offered the attractive feature of imaging different cell populations in the same anatomical site, by labelling each cell population with a different CEST contrast agent.[36] Like with T1 agents, the use of CEST agents also has been limited by sensitivity issues. Therefore, much effort has been put into the generation of macromolecular and nanoparticle-based CEST agents for molecular imaging and cell tracking purposes.[80–82] A type of nanoformulation that has been receiving most interest in this respect is liposomal-based CEST agents.[82,83] While these nanoformulations of CEST agents were shown to have unique features and the potential for interesting molecular imaging applications, their use as efficient intracellular labels was negated by the finding that upon internalization of liposomal CEST agents, image contrast of these agents is significantly reduced.[84] Nonetheless, particulate CEST agents are still considered of interest in the monitoring of cell-based treatment strategies.[8] In a recent study, Chan et al[85] demonstrated the use of a liposomal CEST agent as a nanosensor for monitoring survival of transplanted cells. In this study, the liposomal CEST agent was encapsulated together with hepatocytes in an alginate hydrogel. Due to the pH-sensitive characteristics of the CEST agent, changes in pH within the hydrogel resulting from cell death could be monitored and used as a measure for cell survival (Figure 4). The authors concluded that since all components used were clinical grade, this approach lends itself for clinical translation. Currently there are, to our knowledge, no reports on severe adverse effects of CEST agents on cell functionality.

FLUORINE-19-BASED NANOPARTICLES

A cell labelling strategy that has been gaining increasing interest in recent years lies within the use of fluorine-19 (^{19}F)-based contrast agents. This non-proton-based imaging strategy offers an important advantage from the fact that ^{19}F is not naturally present in the body, consequently endowing ^{19}F-labelled cells with a highly specific signal.[86] Additionally, ^{19}F MRI allows for robust quantification of labelled cells.[87] These characteristics, together with the fact that biologically inert and stable ^{19}F formulations exist and have already been used in clinical settings as oxygen carriers[88] or ultrasound contrast agent (http://www.fda.gov/NewsEvents/Newsroom/PressAnnouncements/ucm418509.htm) have further promoted this interest for ^{19}F-based cell imaging. However, ^{19}F imaging does require some dedicated hardware on a MRI system, which is usually not routinely available in most MRI centres.

For cell labelling, studies have mainly focused on the use on perfluorocarbons (PFCs).[10] A main advantage of PFCs is that each molecule contains a high number of ^{19}F nuclei, increasing the signalling capacity per molecule. In order to promote biocompatibility and cell loading efficiency, formulations of PFCs used for cell labelling and imaging generally consist of coated nanoemulsions or polymer-based nanoparticles.[10,89,90] A nanoemulsion-based formulation of PFCs was also used in the very recently published first report on ^{19}F-based cell imaging in humans.[39] In this study, dendritic cells (DCs) were labelled with a PFC nanoemulsion formulation, with the purpose of visualizing the DCs after intradermal administration as part of a Phase-I trial for DC-based immunotherapy of Stage-4 colorectal cancer (Figure 5). While through this study basic clinical feasibility of ^{19}F-based cell tracking was demonstrated, the current main concern of ^{19}F-based cell imaging, *i.e.* limited sensitivity, was also highlighted. In this study, three patients received a DC injection dose of 1×10^7 cells which could be reliably detected and quantified 4 h after injection. In contrast, in two patients injected with a DC dose of 1×10^6 cells no reliable detection of the cell transplant was possible. For the patients who received 1×10^7, the calculated average intravoxel cell concentration was between 4×10^5 and 6.25×10^5 cells/voxel. In comparison, in the first reported human application of iron oxide-based cell imaging a significantly lower detection sensitivity of labelled cells was demonstrated.[20] In this study, a detection sensitivity of 2×10^3 cells/voxel was demonstrated. Nonetheless, the report by Ahrens et al[39] is encouraging and will certainly further inspire already ongoing efforts into the development of improved ^{19}F-based cell imaging techniques. These involve efforts to increase cellular uptake by probe modifications or the use of transfection agents that promote cellular uptake of particles,[91–93] probe modifications that increase the signalling capacity per molecule,[94,95] and hardware and software developments.[37]

NANOPARTICLE CHARACTERISTICS THAT MAY AFFECT CELL LABELLING EFFICIENCY AND TOXICITY

For nanoparticles to be used for cell labelling purposes, main requirements that should be met are biocompatibility, stability and high contrast generating properties. In the past years various advances in nanotechnology have increased the possibilities in producing a large variety of nanoparticles towards this end. However, various studies have also demonstrated that in practice, limitations regarding these issues are still encountered. In the next paragraphs, we will highlight some of these findings in which specific nanoparticle characteristics are responsible for, sometimes unexpected, effects on cell labelling and/or imaging efficiency and cellular toxicity. In some cases, however, these effects seem to be strongly cell type dependent.

Effects of nanoparticle size

The effect of nanoparticle size on its performance as an intracellular label has been extensively studied and described for iron oxide particles.[96–101] In general, with increasing particle size (up to several microns) more efficient cellular uptake and signalling capacity have been observed. However, also some contradictory results have been reported, where smaller particles showed higher labelling efficiency.[102] Effects of particle size have also been related to some adverse consequences, *i.e.* reduced migration capacity of DCs.[103] In this study, it was shown that migration of DCs labelled with iron oxide nanoparticles was reduced compared with unlabelled cells. The reduction in migration capacity was stronger for larger particles (0.9 μm) compared with smaller particles (80–120 nm). Reduced migratory capacity or cell motility has also been described for iron oxide-labelled neural stem cells and mesenchymal stem cells.[49,104] However, migratory capacity was restored following active exocytosis of the iron oxide nanoparticles. The speed of exocytosis has also been reported to be dependent on nanoparticle size.[105] In a study by Xu et al[106] larger PLGA-encapsulated iron oxide nanoparticles had a 3-fold longer retention in mesenchymal stem cells compared with smaller iron oxide nanoparticles. Active exocytosis has also been reported for various other types of nanoparticles[107–109] and can occur *via* lysosome secretion, vesicle-related secretion and non-vesicle-related secretion.[105] Release of nanoparticles either by active exocytosis or following cell death is considered one of the main disadvantages of the use of nanoparticles for cell labelling and imaging. The released nanoparticles can reside for a long time or be taken up by other cells and thus create a contrast agent-related signal that is not related to the presence of the transplanted cell itself.[51,71,110–113] In the study by Guenoun et al,[71] it was shown that prolonged retention of released cell label is dependent on nanoparticle characteristics. In this study, a comparison was made between iron oxide nanoparticles and Gd–liposomes (liposomes containing gadopentetate dimeglumine in the water phase) as cell labelling agents for monitoring the *in vivo* fate of transplanted cells. Both viable and non-viable cells were injected subcutaneously and monitored over time by MRI. For cells labelled with Gd–liposomes, the cell-associated signalling effect disappeared rapidly when non-viable cells were injected, while the signalling effect of non-viable cells labelled with iron oxide persisted for a long time (Figure 3).

For MnO particles similar observations regarding the effect of particle size on cellular uptake efficiency and signalling capacity were made in a study by Létourneau et al.[35] In this study, small and ultrasmall MnO particles were generated and used for cell labelling.

Figure 2. Limited signal specificity of the iron oxide-labelled cells injected intramyocardially in a porcine myocardial infarction model. The left panel shows gradient echo scan, before injection of iron oxide-labelled cells. The middle panel shows the same slice after injection with 0.1, 1 or 4×10^6 iron oxide-labelled cells. The right panel shows a similar series of injections in remote, non-infarcted myocardium. Although the cell injections create larger areas of signal voids in the middle panel, their precise location cannot be determined because of the signal voids induced by the presence of haemoglobin degradation products. Bar indicates 0.5 cm. Reprinted from van den Bos et al[47] with permission from Oxford University Press.

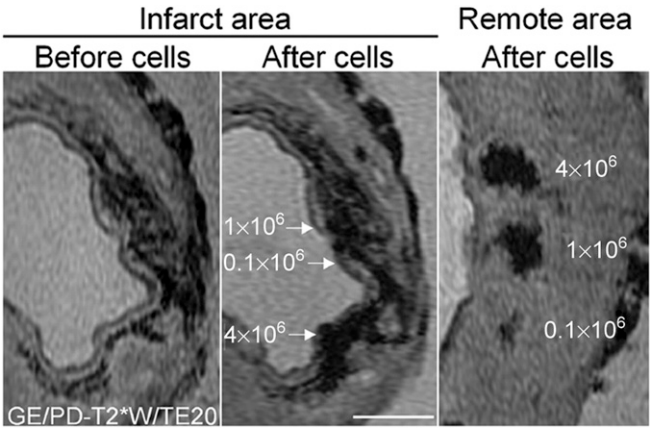

Analogous to observations with iron oxide particles, the larger MnO particles exhibit more efficient cellular uptake. In suspension, the larger particles also exhibited higher relaxivity per Mn atom. Upon internalization into cells, however, the relaxation effect produced by Mn was not anymore different between these two formulations. The likely explanation for this phenomenon is that during endocytosis of the ultrasmall particles, clustering of these particles in endosomes occurred, which apparently resulted in the same net relaxation effect obtained with the larger particles. However, because cellular uptake of the larger particles was more efficient resulting in a higher total cell load on a per cell basis, the larger particles showed superior signalling capacity. A similar effect of intracellular clustering on relaxation properties was found for iron oxide-based nanoparticles.[114] As a negative effect of larger particle size, the authors found a higher toxicity level, reflected in reduced cell viability, for the larger particles than for the smaller particles.[35] The maximal tolerated dose for labelling, that is without affecting cell viability, was approximately two-fold higher for the smaller particles.

To our knowledge, particle size in and of itself has in general not been reported as a major factor affecting cellular function. In general, iron oxide particles are considered as safe for cell labelling with little to no cellular toxicity, at doses relevant for cell labelling. Generally, adverse effects have only been observed at doses exceeding 100 $\mu g\,ml^{-1}$.[115] However, several studies did show negative effects on cellular function following labelling with iron oxide particles at lower doses, including negative effects on multilineage differentiation capacity,[116] migratory capacity,[104] altered cytokine production[117] or cell survival.[118] In a review by Singh et al,[114] the various mechanisms by which iron oxide agents can exert adverse effects on cell function have been discussed, and include effects on membrane integrity, mitochondrial function, generation of reactive oxygen species and DNA damage. In many cases, the toxic effects are dose dependent and related to specific nanoparticle composition aspects.[119] Composition has been shown to be clearly related to potential adverse effects and in general for their performance as cell labelling agent for a large variety of nanoparticle as also illustrated in the section on nanoparticle composition.

Effects of nanoparticle composition

A key aspect of nanoparticles is that they offer a large variability regarding their composition, both in terms of core composition and shell composition. Therefore, nanoparticles can theoretically be generated with a specific purpose in mind, for instance with the goal to be used as a cell labelling agent. The ideal cell labelling agent would have to fulfil the following main requirements: excellent dispersion and stability in physiological fluids and environments, efficient incorporation into cells, high signalling capabilities and excellent biocompatibility. Various studies on the use of nanoparticles as a cell labelling agent have demonstrated that in practice the generation of a nanoparticle that fulfils all these requirements is apparently not so straightforward.

Coating of nanoparticles must provide a good stability to its dispersion and containment of the metal ions that generate the signalling effect. This is important to maintain the signalling properties and to prevent adverse effects caused by free metal atoms, which have been shown to cause cytotoxic effects. For loosely bound coatings such as with the much used dextrans, particle degradation in the presence of an acidic environment, such as in endosomes and lysosomes, has been reported.[120] For iron oxide particles, this was shown to result in rapid modification of the magnetic properties and hampering of long-term follow-up by MRI. Additionally, following degradation of the particle, metal atoms can subsequently leach out into the cytosol causing unwanted cellular effects. Negative effects of leached metal atoms have been shown for iron, gadolinium and manganese.[73,78,115,120] Generally, the observed effects were strongly dose dependent and also connected to uptake efficiency. In various studies, it was also shown that next to uptake efficiency of particles, the extent of the adverse effects could also be strongly cell type dependent.[78,99,121,122] Because of these findings there is a continued effort in trying to generate more stable particles and/or particles with an improved balance between core composition and coating.[77,114,123–125] In our group, we made the observation that for a liposomal encapsulated gadolinium particle, adverse effects on cellular functionality was more directly associated with the liposomal capsule than with the chelated gadolinium molecules.[31] The maximal tolerated dose of the cell label was identical for Gd-encapsulated liposomes as for empty liposomes. In order to promote efficient cellular uptake, we had chosen to generate the liposomes in such a way that they would have a net positive surface charge. As demonstrated in the article, such a formulation did indeed allow for highly efficient uptake of the particles. However, the aspect that promoted cellular uptake was most likely also responsible for the observed dose-dependent

Figure 3. Monitoring the cellular status of cells by situation-dependent contrast behaviour of Gd. MSCs were labelled with either Gd–liposomes or iron oxide particles and an optical reporter gene (firefly luciferase). Following labelling, cell populations were split in two identical samples. One part was then submitted to repeated freeze-thawing to generate non-viable intact cells. Dual-labelled cells were injected intramuscularly into the lower back of rats, *i.e.* viable labelled cells on the left side and non-viable cells on the right side. Rats were imaged by MRI (3.0 T) and bioluminescent imaging at several time points over a period of 2 weeks. (a) SPIO–MSCs caused a signal void (hypointensity), regardless of the cell viability. In the acute post-transplantation stage, no substantial differences in visual appearance were detected between viable and non-viable SPIO-MSCs. (b) Viable Gd–MSCs showed a different dynamic signal behaviour compared with non-viable MSCs. Immediately post-transplantation, viable MSCs were consistently detected as a hypointense area on T_1 weighted scans ("quenched signal intensity"), whereas a similar density of non-viable Gd–MSCs resulted in increased signal intensity (hyperintensity) at the injection site. In contrast to SPIO–MSCs, hyperintense signal from non-viable Gd–MSCs had already resolved after 2 h post-transplantation. An increased signal intensity on BLI images reflects the cell proliferation that contributed to the tracer dilution observed by MRI.T1W, T_1 weighted; T2*W, T_2^* weighted; BLI, bioluminescence imaging; MSCs, mesenchymal stem cells. Reprinted from Guenoun et al[71] with permission from John Wiley and Sons.

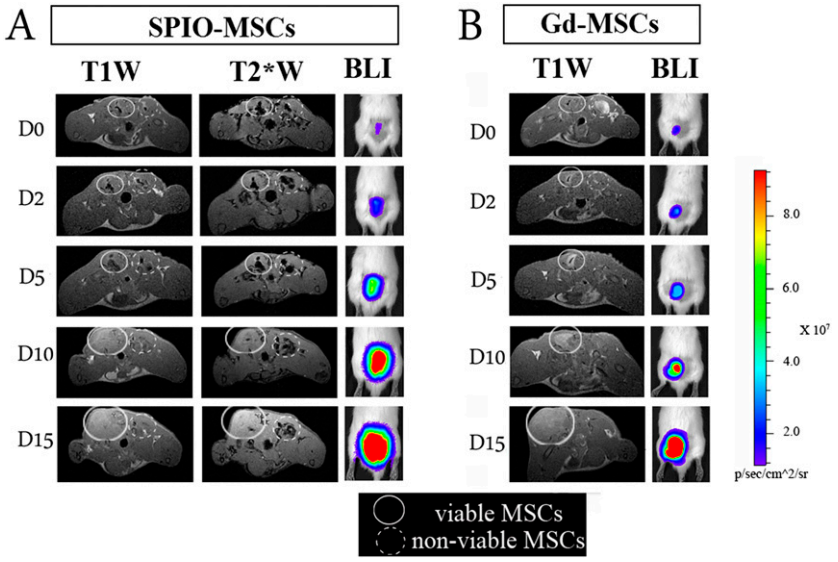

adverse effect. Cationic lipids have been described for their potential to negatively affect cellular function.[126] As an additional positive feature, we did find excellent stability of the intracellular cell label at a non-toxic labelling dose of the Gd–liposomes. Total intracellular Gd content, *i.e.* within the total daughter cell population, did not majorly decline over a culture period of 21 days.

Next to stability of the particle, Kim et al[34] demonstrated that particle coating can also directly influence the signalling efficacy of metal-based probes. In this study, on a new type of MnO particle, they showed that coating with mesoporous silica was superior to coating with PEG–phospholipids and dense silica in terms of T1 relaxivity (>10-fold higher). The superior relaxivity of the mesoporous silica-coated nanoparticles was explained by the facilitated access of surrounding water molecules to the core of the particle containing the manganese ions leading to efficient relaxation of the surrounding water molecules. Their study also demonstrated the effect of coating on cellular uptake efficiency. The mesoporous silica coating endowed the MnO particles with a net negative surface charge. With cell membranes typically having a net negative surface charge, interaction between cells and mesoporous particles is less efficient. Therefore, to promote cell uptake of the negatively charged MnO particles additional manipulation of the cells by electroporation was necessary to obtain efficient labelling. Once internalized, however, the label was well retained in mesenchymal stem cells, allowing for *in vivo* tracking of cells transplanted into the brain of mice for more than 2 weeks.

In a study by Kasten et al[127] effects of nanoparticle composition on signalling efficacy and toxicity were demonstrated using human adipose tissue-derived stem cells. In this study, two types of newly synthetized iron oxide nanoparticles were used that were similar regarding particle size and surface charge but differed regarding iron crystal composition and particle coating. Specifically, these particles consisted of a single iron core particle surrounded by a dextran matrix, called nanomag-D-spio, or a multicrystalline iron core surrounded by a starch shell, called bionized nanoferrite (BNF) starch particles. While both particles showed similar cellular uptake efficiency, a clear difference in signalling capacity and cellular toxicity was found. Unfortunately, the BNF particles that had a more beneficial relaxivity also showed more extensive adverse effects on cellular function in terms of multilineage differentiation capability. Similar effects of iron core composition on signalling capacity were also reported by other groups[101] without reporting any significant differences of core composition on cellular function. In a study by van Tilborg et al,[128] effects of particle core composition on signalling properties, incorporation efficiency and cell functionality were shown. In this study, various biocompatible components were used to generate iron oxide-based

Figure 4. Imaging the functional status of cells by lipoCEST nanosensors. (a) MR images of LipoCEST capsules containing hepatocytes. Shown are magnetization transfer-weighted (MTw) images and magnetization transfer ratio (MTR) asymmetry (MTRasym) maps at 2 ppm of various cell samples. "Apoptotic cells": LipoCEST capsules containing hepatocytes before (0 h) and after (12 hrs) addition of 50 μM staurosporine. "Live cells": LipoCEST capsules containing hepatocytes without the addition of staurosporine imaged at time points 0 and 12 h. "Dead cells": LipoCEST capsules containing hepatocytes treated with STS before encapsulation imaged at time points 0 and 12 h. (b) MTRasym for the three groups at 0 h (open bars) and 12 h (solid bars). (c) Fluorescence overlay images of capsules from the STS and control phantoms shown in (a). Samples are stained for live cells (fluorescein diacetate, green), dead cells (propridium iodide, red) and apoptotic cells (Annexin V, blue). Scale bar = 200 μm. ** indicates statistical significance for the difference in measured values. Reprinted from Chan et al[85] with permission from Nature Publishing Group.

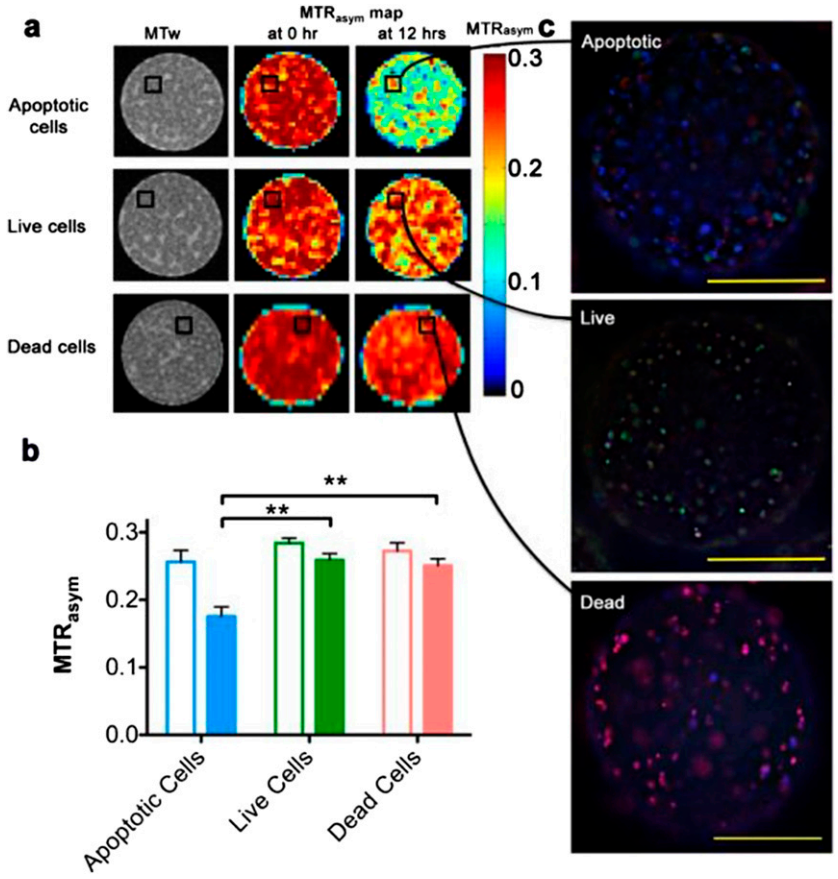

nanoparticles for cell labelling. The various components used to generate the particles were chosen with the goal to obtain particles for efficient cell labelling and imaging. The main surprising finding in this study was that a combination of by itself highly biocompatible components, such as soybean oil, iron oxide phospholipids and polyethylene glycol, resulted in a cytotoxic product. In addition, shelf life of the end product was also significantly reduced following chemical interactions of the components used. In this study, the authors concluded on a negative effect of oxidizing properties of the iron oxide crystals on lipid components of the particle. Furthermore, this study also demonstrated that not only size and surface properties of nanoparticles can strongly influence cellular uptake but also core composition.

In the generation of nanoparticles as a cell labelling agent, apparently various challenges exist in creating an end product that has high signalling capacity, shows efficient cellular uptake and does not negatively affect cell functionality. Therefore, careful testing of all these aspects is required during the evaluation of newly generated products.

CLINICALLY RELEVANT INSIGHTS GAINED FROM PRE-CLINICAL STUDIES AND CLINICAL EXPERIENCE WITH CELL TRACKING

Despite the various challenges met, as described in the previous sections, the value of MRI-based cell tracking for the development and use of cell-based treatment strategies was, amongst others, clearly demonstrated with the first published article on the use of cell tracking by MRI in human patients.[20] In this study, tumour antigen-containing DCs were labelled with iron oxide nanoparticles or ^{111}In-oxine and coinjected into lymph nodes of 10 patients with melanoma under ultrasound guidance. The patients subsequently underwent MRI and scintigraphy, by which the labelled DC vaccine could be visualized. Not only did the study show feasibility of such an approach, the study also demonstrated, owing to the high level of anatomical information obtained with MRI, that in four out of eight

Figure 5. *In vivo* imaging of dendritic cells (DCs) labelled with fluorine-19 (^{19}F) nanoparticles injected intradermally into quadriceps of patients with colorectal cancer. In these patients, approximately 1×10^7 labelled cells were injected. (a) A representative ^{19}F MRS spectrum of patient at 4 h post inoculation. The DCs appear as a single narrow peak. "Reference" is from an external tube containing triflouroacetic acid placed alongside the patient. (b) Axial composite ^{19}F/^{1}H images of the right thigh at 4 h post inoculation in three patients, a 53-year-old female (left), a 45-year-old female (middle) and a 61-year-old male (right), where the DCs are rendered in "hot-iron" pseudocolor and the ^{1}H anatomy is displayed in greyscale (F, femur; RF, rectus femoris; SFA, superficial femoral artery; LN, inguinal lymph node). (c) The results of the *in vivo* quantification of apparent cell numbers using the ^{19}F MRI data, measured in two patients. By approximately 24 h post inoculation, roughly half of the injected DCs were still present at the injection site. Reprinted from Bonetto et al[39] with permission from John Wiley and Sons.

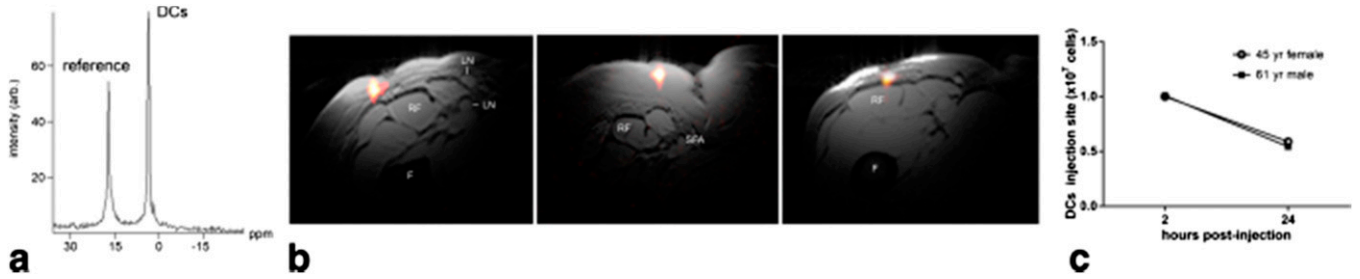

evaluable patients, the injection of the DC vaccine did not occur in the right place. In these four patients, the vaccine was injected into either the surrounding muscle or fat tissue instead of into the target lymph node. Furthermore, imaging of the labelled cells also demonstrated that depending on the patient, higher or larger numbers (1–40%) of the injected cells migrated from the initial target lymph node to surrounding draining lymph nodes. Since this type of therapy is based on direct cell-to-cell interactions between the DC vaccine and T cells in lymph nodes, information such as obtained in this study may be of crucial importance for effective design, execution and monitoring of these kinds of treatment strategies. In the years following this first report on MRI-based cell tracking in humans, a number of other reports on clinical trials were published, in which *in vivo* monitoring of cells labelled with iron oxide nanoparticles was performed.[27–29] These studies in patients with traumatic brain injury, spinal cord injury or diabetes, mainly demonstrated the feasibility of MRI-based cell tracking techniques to monitor delivery and migration of labelled cells. They also provided additional proof on the lack of adverse effects of cell functionality by the labelling procedure, in that cell migration was not impaired or in the case of transplanted pancreatic islets[27] their insulin-producing ability was not impaired. Following these initial four clinical studies, another seven reports on clinical studies with iron oxide-labelled cells appeared. In addition, recently two articles were published describing initial evaluation or preparation of MRI-based cell tracking using PFC nanoparticles[39] and ferumoxytol[56] as cell labelling agents, respectively. Some specifics of these studies and the main findings are summarized in Table 2.

Next to the above mentioned studies, other *in vivo* cell tracking studies (mainly pre-clinical) have provided some valuable insights into the mechanistic aspects of cell-based therapies. For instance, in order for transplanted cells to fulfil their intended function, a first prerequisite is that the cells reach the target site. Connected to this the question arises on what the most efficient route of administration is for a given situation. For stem cell-based therapy of cardiovascular disease, various delivery routes have been contemplated and used, *e.g.* intravenous, intracoronary and intramyocardial injection. *In vivo* tracking studies have revealed that only a limited number of cells reach the infarcted myocardium after intravenous and intracoronary injection.[129,130] Direct intramyocardial injection was shown to result in higher cell delivery efficiency to the infarcted myocardium, however, being a technically quite challenging technique to execute.[131]

Another example of how *in vivo* cell tracking may help in defining the optimal delivery route was demonstrated in a study in rats by Gorelik et al.[132] In this study, homing of glial precursor cell delivery to inflamed brain after intra-arterial injection was studied. To this end, the cells were labelled with iron oxide particles and injected into the carotid artery and their homing to the brain was monitored by MRI. Initial studies showed that without ligation of side-branches of the internal carotid artery, the bulk of injected cells ended up in tissue areas outside the brain. Only after ligation of the side-branches, successful targeting of the injected cells to the brain was achieved (Figure 6). In addition, the investigators also showed that activation of precursor glial cells prior to injection resulted in higher targeting efficiency compared with non-activated cells. This aspect touches upon another important aspect where cell tracking may help in designing effective cell-based treatment strategies. Currently, many cell types are being considered for cell-based therapy; here, the challenge lies in determining which types are most suitable in trying to fulfil criteria regarding therapeutic efficacy, ease of access and practical use.[133] Using fluorine-18 fludeoxyglucose as cell labelling agent and PET imaging, Hofmann et al[129] could demonstrate differences in biodistribution and homing to infarcted myocardium between selected CD34$^+$ bone marrow cells and unselected bone marrow cells when injected intracoronary in patients with myocardial infarction. In another approach, van der Bogt et al[134,135] used bioluminescent imaging of firefly luciferase transduced cells, to compare the efficacy of various cell types for the treatment of myocardial infarction using a murine myocardial infarction model. Most disappointingly, however, the main finding from these studies was the general poor survival in the myocardium of

Figure 6. Real-time monitoring of injection accuracy with MRI. (a) Diagram of procedure with pterygopalatine artery left intact. After ligation of external carotid and occipital arteries, common carotid artery was cannulated and SPIO-labelled cells were infused. (b, c) T_2* weighted MR images of rat brain and surrounding muscles obtained immediately before (b) and after (c) injection demonstrate that vast majority of cells are localized into extracerebral tissue (arrows), with negligible binding within brain. (d) Diagram of procedure with ligation of pterygopalatine artery. All infused cells were perfused into internal carotid artery and localized successfully into ipsilateral hemisphere. (e, f) MR images obtained immediately before (e) and after (f) injection. Arrows indicate area of cell docking. CA, choroidal anterior artery; CCA, common carotid artery; ECA, external carotid artery; ICA, internal carotid artery; MCA, middle cerebral artery; PA, pterygopalatine artery; PCA, posterior cerebral artery. Reprinted from Gorelik et al[132] with permission from the Radiological Society of North America.

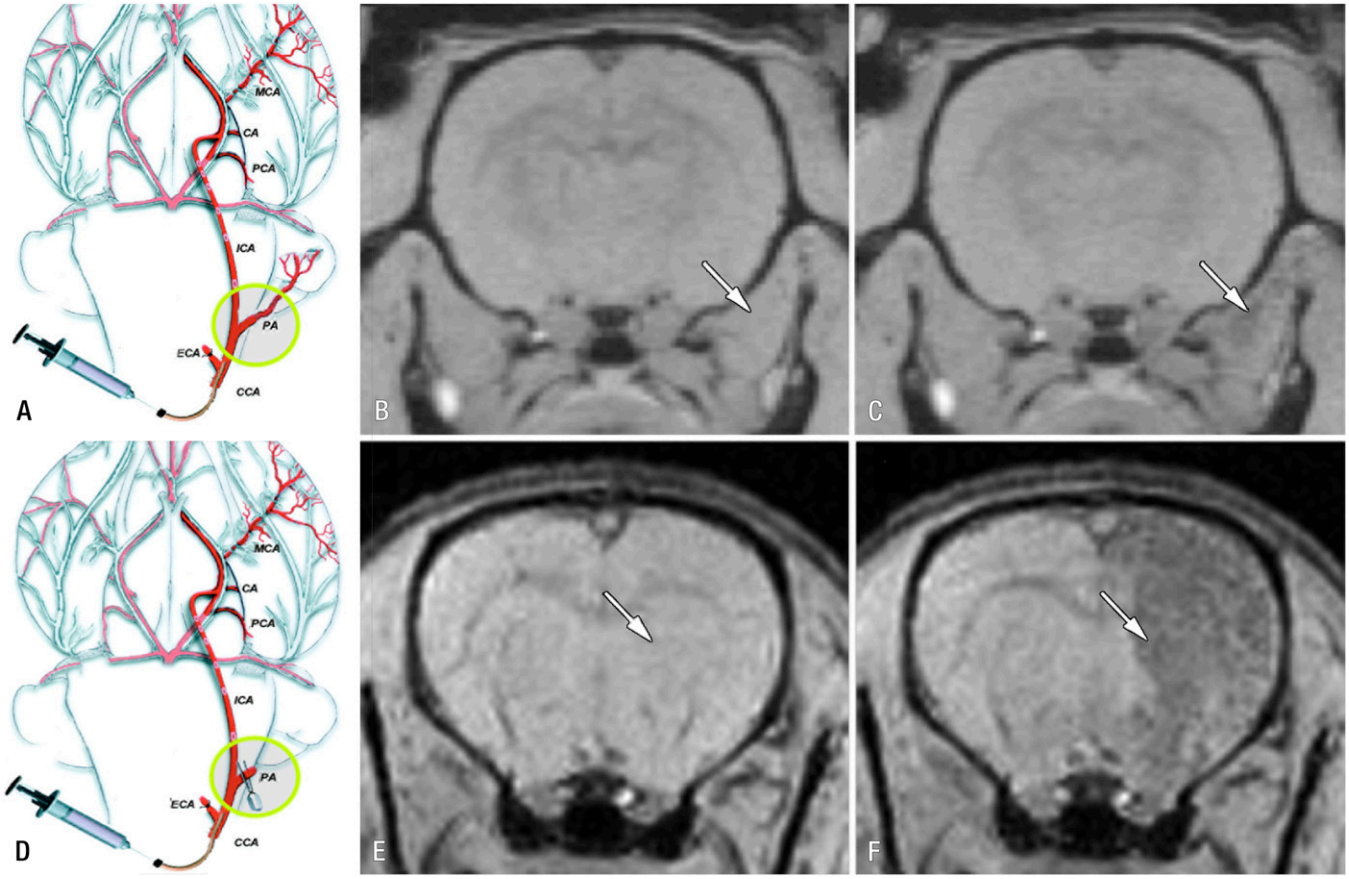

the various cell types tested, including bone marrow mononuclear cells, adipose stromal cells, mesenchymal stem cells, skeletal myoblasts and fibroblasts. Using the same imaging technology, Janowski et al[136] recently demonstrated the site-dependent survival of allogeneic neural progenitor grafts in the brain of mice with a clear involvement of the immune system. Poor graft survival has now been generally accepted as a major hurdle for successful cell therapy in regenerative medicine approaches, therefore much effort is currently put into strategies to improve graft survival.[137–141]

Clearly, *in vivo* cell tracking can provide valuable information for the design and use of cell-based treatment strategies. Unfortunately, current limitations imposed by practical, technical and regulatory issues still prevent widespread clinical use of available imaging technology. Currently no FDA-approved, nanoparticle-based cell labelling agents are available for clinical use. Ferumoxytol, a FDA-approved iron oxide nanoparticle for treatment of anaemia, is now being considered for off-label use as a cell labelling agent in clinical trials.[55,56] To limit the number of regulatory requirements that would have to be fulfilled for this off-label use, an alternative strategy for labelling of mesenchymal stem cells was recently proposed.[55,61] This encompasses labelling of cells *in vivo* instead of *ex vivo* by intravenous injection of ferumoxytol, which is then endocytosed by mesenchymal stromal cells (MSC) in bone marrow. Surprisingly, this technique proved to be highly efficient and superior to *ex vivo* labelling. While this technique was used in an osteochondral defect model, it may be suitable for various other applications and may also be suitable for various other types of nanoparticle-based labels.[142] Of course, for new particles basic safety and signalling efficacy will still have to be proven.

PERSPECTIVES IN CELL TRACKING

Widespread clinical application of cell tracking techniques is at the least, still many years away. However, in coming years much can already be learned from small and large animal models where recent technological developments can further help in

elucidating the mechanisms underlying the success of cell-based therapies. In such pre-clinical studies on cell-based therapies, not only questions regarding accurate delivery of the cell graft can be addressed, but also how the cell grafts function and how therapeutic effect is mediated. These insights can then be used for the design of clinical trials. Next to that, current technology can already be used to address questions regarding the accurate delivery of the graft and migratory behaviour of the cells in specific situations, as has been demonstrated by studies in patients performed so far. The challenge for clinical cell tracking still lies in the development of the ideal technique. No available technique will be able to address all relevant questions. Therefore, depending on the question(s) addressed, the most suitable technique or combination of techniques *i.e.* using multiple modalities, will have to be selected. This will also include the most suitable label for a specific question.

REFERENCES

1. Fischbach MA, Bluestone JA, Lim WA. Cell-based therapeutics: the next pillar of medicine. *Sci Transl Med* 2013; **5**: 179ps7. doi: 10.1126/scitranslmed.3005568
2. Culme-Seymour EJ, Davie NL, Brindley DA, Edwards-Parton S, Mason C. A decade of cell therapy clinical trials (2000-2010). *Regen Med* 2012; **7**: 455–62. doi: 10.2217/rme.12.45
3. Sánchez A, Schimmang T, Garcia-Sancho J. Cell and tissue therapy in regenerative medicine. *Adv Exp Med Biol* 2012; **741**: 89–102. doi: 10.1007/978-1-4614-2098-9_7
4. Hawkins RE, Gilham DE, Debets R, Eshhar Z, Taylor N, Abken H, et al. Development of adoptive cell therapy for cancer: a clinical perspective. *Hum Gene Ther* 2010; **21**: 665–72. doi: 10.1089/hum.2010.086
5. Gioviale MC, Bellavia M, Damiano G, Lo Monte AI. Beyond islet transplantation in diabetes cell therapy: from embryonic stem cells to transdifferentiation of adult cells. *Transplant Proc* 2013; **45**: 2019–24. doi: 10.1016/j.transproceed.2013.01.076
6. Au P, Hursh DA, Lim A, Moos MC Jr, Oh SS, Schneider BS, et al. FDA oversight of cell therapy clinical trials. *Sci Transl Med* 2012; **4**: 149fs31. doi: 10.1126/scitranslmed.3004131
7. Ruggiero A, Thorek DL, Guenoun J, Krestin GP, Bernsen MR. Cell tracking in cardiac repair: what to image and how to image. *Eur Radiol* 2012; **22**: 189–204. doi: 10.1007/s00330-011-2190-7
8. Srivastava AK, Bulte JW. Seeing stem cells at work *in vivo*. *Stem Cell Rev* 2014; **10**: 127–44. doi: 10.1007/s12015-013-9468-x
9. Castaneda RT, Khurana A, Khan R, Daldrup-Link HE. Labeling stem cells with ferumoxytol, an FDA-approved iron oxide nanoparticle. *J Vis Exp* 2011; **4**: e3482. doi: 10.3791/3482
10. Srinivas M, Boehm-Sturm P, Aswendt M, Pracht ED, Figdor CG, de Vries IJ, et al. *In vivo* 19F MRI for cell tracking. *J Vis Exp* 2013; (81): e50802. doi: 10.3791/50802
11. Bernsen MR, Moelker AD, Wielopolski PA, van Tiel ST, Krestin GP. Labelling of mammalian cells for visualisation by MRI. *Eur Radiol* 2010; **20**: 255–74. doi: 10.1007/s00330-009-1540-1
12. Arbab AS, Liu W, Frank JA. Cellular magnetic resonance imaging: current status and future prospects. *Expert Rev Med Devices* 2006; **3**: 427–39. doi: 10.1586/17434440.3.4.427
13. Brader P, Serganova I, Blasberg RG. Non-invasive molecular imaging using reporter genes. *J Nucl Med* 2013; **54**: 167–72. doi: 10.2967/jnumed.111.099788
14. Vandsburger MH, Radoul M, Cohen B, Neeman M. MRI reporter genes: applications for imaging of cell survival, proliferation, migration and differentiation. *NMR Biomed* 2013; **26**: 872–84. doi: 10.1002/nbm.2869
15. Wang Y, Xu C, Ow H. Commercial nanoparticles for stem cell labeling and tracking. *Theranostics* 2013; **3**: 544–60. doi: 10.7150/thno.5634
16. Sutton EJ, Henning TD, Pichler BJ, Bremer C, Daldrup-Link HE. Cell tracking with optical imaging. *Eur Radiol* 2008; **18**: 2021–32. doi: 10.1007/s00330-008-0984-z
17. Aarntzen EH, Srinivas M, Radu CG, Punt CJ, Boerman OC, Figdor CG, et al. *In vivo* imaging of therapy-induced anti-cancer immune responses in humans. *Cell Mol Life Sci* 2013; **70**: 2237–57. doi: 10.1007/s00018-012-1159-2
18. Shapiro EM, Sharer K, Skrtic S, Koretsky AP. *In vivo* detection of single cells by MRI. *Magn Reson Med* 2006; **55**: 242–9. doi: 10.1002/mrm.20718
19. Zhang Z, van den Bos EJ, Wielopolski PA, de Jong-Popijus M, Bernsen MR, Duncker DJ, et al. *In vitro* imaging of single living human umbilical vein endothelial cells with a clinical 3.0-T MRI scanner. *MAGMA* 2005; **18**: 175–85. doi: 10.1007/s10334-005-0108-6
20. de Vries IJ, Lesterhuis WJ, Barentsz JO, Verdijk P, van Krieken JH, Boerman OC, et al. Magnetic resonance tracking of dendritic cells in melanoma patients for monitoring of cellular therapy. *Nat Biotechnol* 2005; **23**: 1407–13. doi: 10.1038/nbt1154
21. Deligianni X, Jirák D, Berková Z, Hájek M, Scheffler K, Bieri O. *In vivo* visualization of cells labeled with superparamagnetic iron oxides by a sub-millisecond gradient echo sequence. *MAGMA* 2014; **27**: 329–37. doi: 10.1007/s10334-013-0422-3
22. Janowski M, Walczak P, Kropiwnicki T, Jurkiewicz E, Domanska-Janik K, Bulte JW, et al. Long-term MRI cell tracking after intraventricular delivery in a patient with global cerebral ischemia and prospects for magnetic navigation of stem cells within the CSF. *PLoS One* 2014; **9**: e97631. doi: 10.1371/journal.pone.0097631
23. Jozwiak S, Habich A, Kotulska K, Sarnowska A, Kropiwnicki T, Janowski M, et al. Intracerebroventricular transplantation of cord blood-derived neural progenitors in a child with severe global brain ischemic injury. *Cell Med* 2010; **1**: 71–88.
24. Karussis D, Karageorgiou C, Vaknin-Dembinsky A, Gowda-Kurkalli B, Gomori JM, Kassis I, et al. Safety and immunological effects of mesenchymal stem cell transplantation in patients with multiple sclerosis and amyotrophic lateral sclerosis. *Arch Neurol* 2010; **67**: 1187–94. doi: 10.1001/archneurol.2010.248
25. Richards JM, Shaw CA, Lang NN, Williams MC, Semple SI, MacGillivray TJ, et al. *In vivo* mononuclear cell tracking using superparamagnetic particles of iron oxide: feasibility and safety in humans. *Circ Cardiovasc Imaging* 2012; **5**: 509–17. doi: 10.1161/CIRCIMAGING.112.972596
26. Saudek F, Jirák D, Girman P, Herynek V, Dezortová M, Kríz J, et al. Magnetic resonance imaging of pancreatic islets transplanted into the liver in humans. *Transplantation* 2010; **90**: 1602–6. doi: 10.1097/TP.0b013e3181ffba5e
27. Toso C, Vallee JP, Morel P, Ris F, Demuylder-Mischler S, Lepetit-Coiffe M, et al. Clinical magnetic resonance imaging of pancreatic islet grafts after iron nanoparticle labeling. *Am J Transpl* 2008; **8**:

701–6. doi: 10.1111/j.1600-6143.2007.02120.x
28. Zhu J, Zhou L, XingWu F. Tracking neural stem cells in patients with brain trauma. *N Engl J Med* 2006; **355**: 2376–8. doi: 10.1056/NEJMc055304
29. Callera F, de Melo CM. Magnetic resonance tracking of magnetically labeled autologous bone marrow CD34+ cells transplanted into the spinal cord *via* lumbar puncture technique in patients with chronic spinal cord injury: CD34+ cells' migration into the injured site. *Stem Cells Dev* 2007; **16**: 461–6. doi: 10.1089/scd.2007.0083
30. Figueiredo S, Cutrin JC, Rizzitelli S, De Luca E, Moreira JN, Geraldes CF, et al. MRI tracking of macrophages labeled with glucan particles entrapping a water insoluble paramagnetic Gd-based agent. *Mol Imaging Biol* 2013; **15**: 307–15. doi: 10.1007/s11307-012-0603-x
31. Guenoun J, Koning GA, Doeswijk G, Bosman L, Wielopolski PA, Krestin GP, et al. Cationic Gd-DTPA liposomes for highly efficient labeling of mesenchymal stem cells and cell tracking with MRI. *Cell Transpl* 2012; **21**: 191–205. doi: 10.3727/096368911X593118
32. Aspord C, Laurin D, Janier MF, Mandon CA, Thivolet C, Villiers C, et al. Paramagnetic nanoparticles to track and quantify *in vivo* immune human therapeutic cells. *Nanoscale* 2013; **5**: 11409–15. doi: 10.1039/c3nr34240a
33. Sterenczak KA, Meier M, Glage S, Meyer M, Willenbrock S, Wefstaedt P, et al. Longitudinal MRI contrast enhanced monitoring of early tumour development with manganese chloride (MnCl2) and superparamagnetic iron oxide nanoparticles (SPIOs) in a CT1258 based *in vivo* model of prostate cancer. *BMC Cancer* 2012; **12**: 284. doi: 10.1186/1471-2407-12-284
34. Kim T, Momin E, Choi J, Yuan K, Zaidi H, Kim J, et al. Mesoporous silica-coated hollow manganese oxide nanoparticles as positive T1 contrast agents for labeling and MRI tracking of adipose-derived mesenchymal stem cells. *J Am Chem Soc* 2011; **133**: 2955–61. doi: 10.1021/ja1084095
35. Létourneau M, Tremblay M, Faucher L, Rojas D, Chevallier P, Gossuin Y, et al. MnO-labeled cells: positive contrast enhancement in MRI. *J Phys Chem B* 2012; **116**: 13228–38. doi: 10.1021/jp3032918
36. Ferrauto G, Delli Castelli D, Terreno E, Aime S. *In vivo* MRI visualization of different cell populations labeled with PARACEST agents. *Magn Reson Med* 2013; **69**: 1703–11. doi: 10.1002/mrm.24411
37. Amiri H, Srinivas M, Veltien A, van Uden MJ, de Vries IJ, Heerschap A. Cell tracking using (19)F magnetic resonance imaging: technical aspects and challenges towards clinical applications. *Eur Radiol* 2015; **25**: 726–35. doi: 10.1007/s00330-014-3474-5
38. Bonetto F, Srinivas M, Heerschap A, Mailliard R, Ahrens ET, Figdor CG, et al. A novel (19)F agent for detection and quantification of human dendritic cells using magnetic resonance imaging. *Int J Cancer* 2011; **129**: 365–73. doi: 10.1002/ijc.25672
39. Ahrens ET, Helfer BM, O'Hanlon CF, Schirda C. Clinical cell therapy imaging using a perfluorocarbon tracer and fluorine-19 MRI. *Magn Reson Med* 2014; **72**: 1696–701. doi: 10.1002/mrm.25454
40. Bulte JW, Ma LD, Magin RL, Kamman RL, Hulstaert CE, Go KG, et al. Selective MR imaging of labeled human peripheral blood mononuclear cells by liposome mediated incorporation of dextran-magnetite particles. *Magn Reson Med* 1993; **29**: 32–7. doi: 10.1002/mrm.1910290108
41. Norman AB, Thomas SR, Pratt RG, Lu SY, Norgren RB. Magnetic resonance imaging of neural transplants in rat brain using a superparamagnetic contrast agent. *Brain Res* 1992; **594**: 279–83. doi: 10.1016/0006-8993(92)91135-2
42. Bulte JW, Kraitchman DL. Iron oxide MR contrast agents for molecular and cellular imaging. *NMR Biomed* 2004; **17**: 484–99. doi: 10.1002/nbm.924
43. Li L, Jiang W, Luo K, Song H, Lan F, Wu Y, et al. Superparamagnetic iron oxide nanoparticles as MRI contrast agents for non-invasive stem cell labeling and tracking. *Theranostics* 2013; **3**: 595–615. doi: 10.7150/thno.5366
44. Daldrup-Link HE, Meier R, Rudelius M, Piontek G, Piert M, Metz S, et al. *In vivo* tracking of genetically engineered, anti-HER2/neu directed natural killer cells to HER2/neu positive mammary tumors with magnetic resonance imaging. *Eur Radiol* 2005; **15**: 4–13. doi: 10.1007/s00330-004-2526-7
45. Frank JA, Zywicke H, Jordan EK, Mitchell J, Lewis BK, Miller B, et al. Magnetic intracellular labeling of mammalian cells by combining (FDA-approved) superparamagnetic iron oxide MR contrast agents and commonly used transfection agents. *Acad Radiol* 2002; **9** (Suppl 2): S484–7.
46. Bulte JW. *In vivo* MRI cell tracking: clinical studies. *AJR Am J Roentgenol* 2009; **193**: 314–25. doi: 10.2214/AJR.09.3107
47. van den Bos EJ, Baks T, Moelker AD, Kerver W, van Geuns RJ, van der Giessen WJ, et al. Magnetic resonance imaging of haemorrhage within reperfused myocardial infarcts: possible interference with iron oxide-labelled cell tracking? *Eur Heart J* 2006; **27**: 1620–6. doi: 10.1093/eurheartj/ehl059
48. Terrovitis J, Stuber M, Youssef A, Preece S, Leppo M, Kizana E, et al. Magnetic resonance imaging overestimates ferumoxide-labeled stem cell survival after transplantation in the heart. *Circulation* 2008; **117**: 1555–62. doi: 10.1161/CIRCULATIONAHA.107.732073
49. Cromer Berman SM, Kshitiz, Wang CJ, Orukari I, Levchenko A, Bulte JW, et al. Cell motility of neural stem cells is reduced after SPIO-labeling, which is mitigated after exocytosis. *Magn Reson Med* 2013; **69**: 255–62. doi: 10.1002/mrm.24216
50. Wang Q, Li K, Quan Q, Zhang G. R2* and R2 mapping for quantifying recruitment of superparamagnetic iron oxide-tagged endothelial progenitor cells to injured liver: tracking *in vitro* and *in vivo*. *Int J Nanomedicine* 2014; **9**: 1815–22. doi: 10.2147/IJN.S58269
51. van Buul GM, Kotek G, Wielopolski PA, Farrell E, Bos PK, Weinans H, et al. Clinically translatable cell tracking and quantification by MRI in cartilage repair using superparamagnetic iron oxides. *PLoS One* 2011; **6**: e17001. doi: 10.1371/journal.pone.0017001
52. Girard OM, Ramirez R, McCarty S, Mattrey RF. Toward absolute quantification of iron oxide nanoparticles as well as cell internalized fraction using multiparametric MRI. *Contrast Media Mol Imaging*. 2012; **7**: 411–17. doi: 10.1002/cmmi.1467
53. Kotek G, van Tiel ST, Wielopolski PA, Houston GC, Krestin GP, Bernsen MR. Cell quantification: evolution of compartmentalization and distribution of iron-oxide particles and labeled cells. *Contrast Media Mol Imaging* 2012; **7**: 195–203. doi: 10.1002/cmmi.481
54. Ruggiero A, Guenoun J, Smit H, Doeswijk GN, Klein S, Krestin GP, et al. *In vivo* MRI mapping of iron oxide-labeled stem cells transplanted in the heart. *Contrast Media Mol Imaging* 2013; **8**: 487–94. doi: 10.1002/cmmi.1582
55. Daldrup-Link HE, Nejadnik H. MR imaging of stem cell transplants in arthritic joints. *J Stem Cell Res Ther* 2014; **4**: 165. doi: 10.4172/2157-7633.1000165
56. Gutova M, Frank JA, D'Apuzzo M, Khankaldyyan V, Gilchrist MM, Annala AJ, et al. Magnetic resonance imaging tracking of ferumoxytol-labeled human neural stem cells: studies leading to clinical use. *Stem*

Cells Transl Med 2013; **2**: 766–75. doi: 10.5966/sctm.2013-0049

57. Bridot JL, Stanicki D, Laurent S, Boutry S, Gossuin Y, Leclère P, et al. New carboxysilane-coated iron oxide nanoparticles for nonspecific cell labelling. *Contrast Media Mol Imaging* 2013; **8**: 466–74. doi: 10.1002/cmmi.1552
58. Liu J, Wang L, Cao J, Huang Y, Lin Y, Wu X, et al. Functional investigations on embryonic stem cells labeled with clinically translatable iron oxide nanoparticles. *Nanoscale* 2014; **6**: 9025–33. doi: 10.1039/c4nr01004c
59. Leder A, Raschzok N, Schmidt C, Arabacioglu D, Butter A, Kolano S, et al. Micron-sized iron oxide-containing particles for microRNA-targeted manipulation and MRI-based tracking of transplanted cells. *Biomaterials* 2015; **51**: 129–37. doi: 10.1016/j.biomaterials.2015.01.065
60. Chapman S, Dobrovolskaia M, Farahani K, Goodwin A, Joshi A, Lee H, et al. Nanoparticles for cancer imaging: the good, the bad, and the promise. *Nano Today* 2013; **8**: 454–60. doi: 10.1016/j.nantod.2013.06.001
61. Khurana A, Nejadnik H, Chapelin F, Lenkov O, Gawande R, Lee S, et al. Ferumoxytol: a new, clinically applicable label for stem-cell tracking in arthritic joints with MRI. *Nanomedicine (Lond)* 2013; **8**: 1969–83. doi: 10.2217/nnm.12.198
62. Rudelius M, Daldrup-Link HE, Heinzmann U, Piontek G, Settles M, Link TM, et al. Highly efficient paramagnetic labelling of embryonic and neuronal stem cells. *Eur J Nucl Med Mol Imaging* 2003; **30**: 1038–44. doi: 10.1007/s00259-002-1110-0
63. Tseng CL, Shih IL, Stobinski L, Lin FH. Gadolinium hexanedione nanoparticles for stem cell labeling and tracking *via* magnetic resonance imaging. *Biomaterials* 2010; **31**: 5427–35. doi: 10.1016/j.biomaterials.2010.03.049
64. Ghaghada KB, Ravoori M, Sabapathy D, Bankson J, Kundra V, Annapragada A. New dual mode gadolinium nanoparticle contrast agent for magnetic resonance imaging. *PLoS One* 2009; **4**: e7628. doi: 10.1371/journal.pone.0007628
65. Nejadnik H, Henning TD, Do T, Sutton EJ, Baehner F, Horvai A, et al. MR imaging features of gadofluorine-labeled matrix-associated stem cell implants in cartilage defects. *PLoS One* 2012; **7**: e49971. doi: 10.1371/journal.pone.0049971
66. Di Corato R, Gazeau F, Le Visage C, Fayol D, Levitz P, Lux F, et al. High-resolution cellular MRI: gadolinium and iron oxide nanoparticles for in-depth dual-cell imaging of engineered tissue constructs. *ACS Nano* 2013; **7**: 7500–12. doi: 10.1021/nn401095p
67. Vivero-Escoto JL, Rieter WJ, Lau H, Huxford-Phillips RC, Lin W. Biodegradable polysilsesquioxane nanoparticles as efficient contrast agents for magnetic resonance imaging. *Small* 2013; **9**: 3523–31. doi: 10.1002/smll.201300198
68. Tran LA, Hernández-Rivera M, Berlin AN, Zheng Y, Sampaio L, Bové C, et al. The use of gadolinium-carbon nanostructures to magnetically enhance stem cell retention for cellular cardiomyoplasty. *Biomaterials* 2014; **35**: 720–6. doi: 10.1016/j.biomaterials.2013.10.013
69. Terreno E, Geninatti Crich S, Belfiore S, Biancone L, Cabella C, Esposito G, et al. Effect of the intracellular localization of a Gd-based imaging probe on the relaxation enhancement of water protons. *Magn Reson Med* 2006; **55**: 491–7. doi: 10.1002/mrm.20793
70. Brekke C, Morgan SC, Lowe AS, Meade TJ, Price J, Williams SC, et al. The *in vitro* effects of a bimodal contrast agent on cellular functions and relaxometry. *NMR Biomed* 2007; **20**: 77–89. doi: 10.1002/nbm.1077
71. Guenoun J, Ruggiero A, Doeswijk G, Janssens RC, Koning GA, Kotek G, et al. *In vivo* quantitative assessment of cell viability of gadolinium or iron-labeled cells using MRI and bioluminescence imaging. *Contrast Media Mol Imaging* 2013; **8**: 165–74.doi: 10.1002/cmmi.1513
72. Nejadnik H, Castillo R, Daldrup-Link HE. Magnetic resonance imaging and tracking of stem cells. *Methods Mol Biol* 2013; **1052**: 167–76. doi: 10.1007/7651_2013_16
73. Zhang S, Jiang Z, Liu X, Zhou L, Peng W. Possible gadolinium ions leaching and MR sensitivity over-estimation in mesoporous silica-coated upconversion nanocrystals. *Nanoscale* 2013; **5**: 8146–55. doi: 10.1039/c3nr01902k
74. Modo M, Beech JS, Meade TJ, Williams SC, Price J. A chronic 1 year assessment of MRI contrast agent-labelled neural stem cell transplants in stroke. *Neuroimage* 2009; **47** (Suppl 2): T133–42. doi: 10.1016/j.neuroimage.2008.06.017
75. Gilad AA, Walczak P, McMahon MT, Na HB, Lee JH, An K, et al. MR tracking of transplanted cells with "positive contrast" using manganese oxide nanoparticles. *Magn Reson Med* 2008; **60**: 1–7. doi: 10.1002/mrm.21622
76. Yamada M, Gurney PT, Chung J, Kundu P, Drukker M, Smith AK, et al. Manganese-guided cellular MRI of human embryonic stem cell and human bone marrow stromal cell viability. *Magn Reson Med* 2009; **62**: 1047–54. doi: 10.1002/mrm.22071
77. Xiao J, Tian XM, Yang C, Liu P, Luo NQ, Liang Y, et al. Ultrahigh relaxivity and safe probes of manganese oxide nanoparticles for *in vivo* imaging. *Sci Rep* 2013; **3**: 3424. doi: 10.1038/srep03424
78. Yu C, Zhou Z, Wang J, Sun J, Liu W, Sun Y, et al. In depth analysis of apoptosis induced by silica coated manganese oxide nanoparticles *in vitro*. *J Hazard Mater* 2015; **283**: 519–28. doi: 10.1016/j.jhazmat.2014.09.060
79. Bellusci M, La Barbera A, Padella F, Mancuso M, Pasquo A, Grollino MG, et al. Biodistribution and acute toxicity of a nanofluid containing manganese iron oxide nanoparticles produced by a mechanochemical process. *Int J Nanomedicine* 2014; **9**: 1919–29. doi: 10.2147/IJN.S56394
80. Vinogradov E, Sherry AD, Lenkinski RE. CEST: from basic principles to applications, challenges and opportunities. *J Magn Reson* 2013; **229**: 155–72. doi: 10.1016/j.jmr.2012.11.024
81. Ferrauto G, Carniato F, Tei L, Hu H, Aime S, Botta M. MRI nanoprobes based on chemical exchange saturation transfer: Ln (III) chelates anchored on the surface of mesoporous silica nanoparticles. *Nanoscale* 2014; **6**: 9604–7. doi: 10.1039/c4nr02753a
82. Castelli DD, Terreno E, Longo D, Aime S. Nanoparticle-based chemical exchange saturation transfer (CEST) agents. *NMR Biomed* 2013; **26**: 839–49. doi: 10.1002/nbm.2974
83. Chan KW, Bulte JW, McMahon MT. Diamagnetic chemical exchange saturation transfer (diaCEST) liposomes: physicochemical properties and imaging applications. *Wiley Interdiscip Rev Nanomed Nanobiotechnol* 2014; **6**: 111–24. doi: 10.1002/wnan.1246
84. Kok MB, Hak S, Mulder WJ, van der Schaft DW, Strijkers GJ, Nicolay K. Cellular compartmentalization of internalized paramagnetic liposomes strongly influences both T1 and T2 relaxivity. *Magn Reson Med* 2009; **61**: 1022–32. doi: 10.1002/mrm.21910
85. Chan KW, Liu G, Song X, Kim H, Yu T, Arifin DR, et al. MRI-detectable pH nanosensors incorporated into hydrogels for *in vivo* sensing of transplanted-cell viability. *Nat Mater* 2013; **12**: 268–75. doi: 10.1038/nmat3525
86. Ruiz-Cabello J, Barnett BP, Bottomley PA, Bulte JW. Fluorine (19F) MRS and MRI in biomedicine. *NMR Biomed* 2011; **24**: 114–29. doi: 10.1002/nbm.1570
87. Srinivas M, Heerschap A, Ahrens ET, Figdor CG, de Vries IJ. (19)F MRI for quantitative *in vivo* cell tracking. *Trends Biotechnol* 2010;

28: 363–70. doi: 10.1016/j.tibtech.2010.04.002
88. Zarif L, Postel M, Trevino L, Riess JG, Valla A, Follana R. Biodistribution and excretion of a mixed fluorocarbon-hydrocarbon "dowel" emulsion as determined by 19F NMR. *Artif Cells Blood Substit Immobil Biotechnol* 1994; **22**: 1193–8. doi: 10.3109/10731199409138815
89. Helfer BM, Balducci A, Nelson AD, Janjic JM, Gil RR, Kalinski P, et al. Functional assessment of human dendritic cells labeled for *in vivo* (19)F magnetic resonance imaging cell tracking. *Cytotherapy* 2010; **12**: 238–50. doi: 10.3109/14653240903446902
90. Srinivas M, Cruz LJ, Bonetto F, Heerschap A, Figdor CG, de Vries IJ. Customizable, multi-functional fluorocarbon nanoparticles for quantitative *in vivo* imaging using 19F MRI and optical imaging. *Biomaterials* 2010; **31**: 7070–7. doi: 10.1016/j.biomaterials.2010.05.069
91. Srinivas M, Boehm-Sturm P, Figdor CG, de Vries IJ, Hoehn M. Labeling cells for *in vivo* tracking using (19)F MRI. *Biomaterials* 2012; **33**: 8830–40. doi: 10.1016/j.biomaterials.2012.08.048
92. Ahrens ET, Zhong J. *In vivo* MRI cell tracking using perfluorocarbon probes and fluorine-19 detection. *NMR Biomed* 2013; **26**: 860–71. doi: 10.1002/nbm.2948
93. Waiczies S, Lepore S, Sydow K, Drechsler S, Ku MC, Martin C, et al. Anchoring dipalmitoyl phosphoethanolamine to nanoparticles boosts cellular uptake and fluorine-19 magnetic resonance signal. *Sci Rep* 2015; **5**: 8427. doi: 10.1038/srep08427
94. Chalmers KH, Kenwright AM, Parker D, Blamire AM. 19F-lanthanide complexes with increased sensitivity for 19F-MRI: optimization of the MR acquisition. *Magn Reson Med* 2011; **66**: 931–6. doi: 10.1002/mrm.22881
95. de Vries A, Moonen R, Yildirim M, Langereis S, Lamerichs R, Pikkemaat JA, et al. Relaxometric studies of gadolinium-functionalized perfluorocarbon nanoparticles for MR imaging. *Contrast Media Mol Imaging* 2014; **9**: 83–91. doi: 10.1002/cmmi.1541
96. Shapiro EM, Skrtic S, Koretsky AP. Sizing it up: cellular MRI using micron-sized iron oxide particles. *Magn Reson Med* 2005; **53**: 329–38. doi: 10.1002/mrm.20342
97. Matuszewski L, Persigehl T, Wall A, Schwindt W, Tombach B, Fobker M, et al. Cell tagging with clinically approved iron oxides: feasibility and effect of lipofection, particle size, and surface coating on labeling efficiency. *Radiology* 2005; **235**: 155–61. doi: 10.1148/radiol.2351040094
98. Chen CL, Zhang H, Ye Q, Hsieh WY, Hitchens TK, Shen HH, et al. A new nano-sized iron oxide particle with high sensitivity for cellular magnetic resonance imaging. *Mol Imaging Biol* 2011; **13**: 825–39. doi: 10.1007/s11307-010-0430-x
99. van Tiel ST, Wielopolski PA, Houston GC, Krestin GP, Bernsen MR. Variations in labeling protocol influence incorporation, distribution and retention of iron oxide nanoparticles into human umbilical vein endothelial cells. *Contrast Media Mol Imaging*. 2010; **5**: 247–57. doi: 10.1002/cmmi.379
100. Saito S, Tsugeno M, Koto D, Mori Y, Yoshioka Y, Nohara S, et al. Impact of surface coating and particle size on the uptake of small and ultrasmall superparamagnetic iron oxide nanoparticles by macrophages. *Int J Nanomedicine* 2012; **7**: 5415–21. doi: 10.2147/IJN.S33709
101. Trekker J, Leten C, Struys T, Lazenka VV, Argibay B, Micholt L, et al. Sensitive *in vivo* cell detection using size-optimized superparamagnetic nanoparticles. *Biomaterials* 2014; **35**: 1627–35. doi: 10.1016/j.biomaterials.2013.11.006
102. Hansen L, Hansen AB, Mathiasen AB, Ng M, Bhakoo K, Ekblond A, et al. Ultrastructural characterization of mesenchymal stromal cells labeled with ultrasmall superparamagnetic iron-oxide nanoparticles for clinical tracking studies. *Scand J Clin Lab Invest* 2014; **74**: 437–46. doi: 10.3109/00365513.2014.900698
103. de Chickera SN, Snir J, Willert C, Rohani R, Foley R, Foster PJ, et al. Labelling dendritic cells with SPIO has implications for their subsequent *in vivo* migration as assessed with cellular MRI. *Contrast Media Mol Imaging* 2011; **6**: 314–27. doi: 10.1002/cmmi.433
104. Schafer R, Kehlbach R, Müller M, Bantleon R, Kluba T, Ayturan M, et al. Labeling of human mesenchymal stromal cells with superparamagnetic iron oxide leads to a decrease in migration capacity and colony formation ability. *Cytotherapy* 2009; **11**: 68–78. doi: 10.1080/14653240802666043
105. Oh N, Park JH. Endocytosis and exocytosis of nanoparticles in mammalian cells. *Int J Nanomedicine* 2014; **9** (Suppl 1): 51–63. doi: 10.2147/IJN.S26592
106. Xu C, Miranda-Nieves D, Ankrum JA, Matthiesen ME, Phillips JA, Roes I, et al. Tracking mesenchymal stem cells with iron oxide nanoparticle loaded poly(lactide-co-glycolide) microparticles. *Nano Lett* 2012; **12**: 4131–9. doi: 10.1021/nl301658q
107. Bible E, Dell'Acqua F, Solanky B, Balducci A, Crapo PM, Badylak SF, et al. Non-invasive imaging of transplanted human neural stem cells and ECM scaffold remodeling in the stroke-damaged rat brain by (19)F- and diffusion-MRI. *Biomaterials* 2012; **33**: 2858–71. doi: 10.1016/j.biomaterials.2011.12.033
108. Chu Z, Huang Y, Tao Q, Li Q. Cellular uptake, evolution, and excretion of silica nanoparticles in human cells. *Nanoscale* 2011; **3**: 3291–9. doi: 10.1039/c1nr10499c
109. Luciani N, Wilhelm C, Gazeau F. The role of cell-released microvesicles in the intercellular transfer of magnetic nanoparticles in the monocyte/macrophage system. *Biomaterials* 2010; **31**: 7061–9. doi: 10.1016/j.biomaterials.2010.05.062
110. Huang Z, Li C, Yang S, Xu J, Shen Y, Xie X, et al. Magnetic resonance hypointensive signal primarily originates from extracellular iron particles in the long-term tracking of mesenchymal stem cells transplanted in the infarcted myocardium. *Int J Nanomedicine* 2015; **10**: 1679–90. doi: 10.2147/IJN.S77858
111. Winter EM, Hogers B, van der Graaf LM, Gittenberger-de Groot AC, Poelmann RE, van der Weerd L. Cell tracking using iron oxide fails to distinguish dead from living transplanted cells in the infarcted heart. *Magn Reson Med* 2010; **63**: 817–21. doi: 10.1002/mrm.22094
112. Pawelczyk E, Jordan EK, Balakumaran A, Chaudhry A, Gormley N, Smith M, et al. *In vivo* transfer of intracellular labels from locally implanted bone marrow stromal cells to resident tissue macrophages. *PLoS One* 2009; **4**: e6712. doi: 10.1371/journal.pone.0006712
113. Gaudet JM, Ribot EJ, Chen Y, Gilbert KM, Foster PJ. Tracking the fate of stem cell implants with fluorine-19 MRI. *PLoS One* 2015; **10**: e0118544. doi: 10.1371/journal.pone.0118544
114. Weis C, Blank F, West A, Black G, Woodward RC, Carroll MR, et al. Labeling of cancer cells with magnetic nanoparticles for magnetic resonance imaging. *Magn Reson Med* 2014; **71**: 1896–905. doi: 10.1002/mrm.24832
115. Singh N, Jenkins GJ, Asadi R, Doak SH. Potential toxicity of superparamagnetic iron oxide nanoparticles (SPION). *Nano Rev* 2010; **1**. doi: 10.3402/nano.v1i0.5358
116. Kostura L, Kraitchman DL, Mackay AM, Pittenger MF, Bulte JW. Feridex labeling of mesenchymal stem cells inhibits chondrogenesis but not adipogenesis or osteogenesis. *NMR Biomed* 2004; **17**: 513–17. doi: 10.1002/nbm.925
117. Siglienti I, Bendszus M, Kleinschnitz C, Stoll G. Cytokine profile of iron-laden

macrophages: implications for cellular magnetic resonance imaging. *J Neuroimmunol* 2006; **173**: 166–73. doi: 10.1016/j.jneuroim.2005.11.011

118. Arbab AS, Yocum GT, Wilson LB, Parwana A, Jordan EK, Kalish H, et al. Comparison of transfection agents in forming complexes with ferumoxides, cell labeling efficiency, and cellular viability. *Mol Imaging* 2004; **3**: 24–32. doi: 10.1162/153535004773861697
119. Kunzmann A, Andersson B, Vogt C, Feliu N, Ye F, Gabrielsson S, et al. Efficient internalization of silica-coated iron oxide nanoparticles of different sizes by primary human macrophages and dendritic cells. *Toxicol Appl Pharmacol* 2011; **253**: 81–93. doi: 10.1016/j.taap.2011.03.011
120. Soenen SJ, Himmelreich U, Nuytten N, Pisanic TR 2nd, Ferrari A, De Cuyper M. Intracellular nanoparticle coating stability determines nanoparticle diagnostics efficacy and cell functionality. *Small* 2010; **6**: 2136–45. doi: 10.1002/smll.201000763
121. Ketkar-Atre A, Struys T, Soenen SJ, Lambrichts I, Verfaillie CM, De Cuyper M, et al. Variability in contrast agent uptake by different but similar stem cell types. *Int J Nanomedicine* 2013; **8**: 4577–91. doi: 10.2147/IJN.S51588
122. Lojk J, Bregar VB, Rajh M, Miš K, Kreft ME, Pirkmajer S, et al. Cell type-specific response to high intracellular loading of polyacrylic acid-coated magnetic nanoparticles. *Int J Nanomedicine* 2015; **10**: 1449–62. doi: 10.2147/IJN.S76134
123. Eamegdool SS, Weible MW 2nd, Pham BT, Hawkett BS, Grieve SM, Chan-ling T. Ultrasmall superparamagnetic iron oxide nanoparticle prelabelling of human neural precursor cells. *Biomaterials* 2014; **35**: 5549–64. doi: 10.1016/j.biomaterials.2014.03.061
124. Tian F, Chen G, Yi P, Zhang J, Li A, Zhang J, et al. Fates of Fe3O4 and Fe3O4@SiO2 nanoparticles in human mesenchymal stem cells assessed by synchrotron radiation-based techniques. *Biomaterials* 2014; **35**: 6412–21. doi: 10.1016/j.biomaterials.2014.04.052
125. Matsushita H, Mizukami S, Sugihara F, Nakanishi Y, Yoshioka Y, Kikuchi K. Multifunctional core-shell silica nanoparticles for highly sensitive (19)F magnetic resonance imaging. *Angew Chem Int Ed Engl* 2014; **53**: 1008–11. doi: 10.1002/anie.201308500
126. Soenen SJ, Brisson AR, De Cuyper M. Addressing the problem of cationic lipid-mediated toxicity: the magnetoliposome model. *Biomaterials* 2009; **30**: 3691–701. doi: 10.1016/j.biomaterials.2009.03.040
127. Kasten A, Grüttner C, Kühn JP, Bader R, Pasold J, Frerich B. Comparative *in vitro* study on magnetic iron oxide nanoparticles for MRI tracking of adipose tissue-derived progenitor cells. *PLoS One* 2014; **9**: e108055. doi: 10.1371/journal.pone.0108055
128. van Tilborg GA, Cormode DP, Jarzyna PA, van der Toorn A, van der Pol SM, van Bloois L, et al. Nanoclusters of iron oxide: effect of core composition on structure, biocompatibility, and cell labeling efficacy. *Bioconjug Chem* 2012; **23**: 941–50. doi: 10.1021/bc200543k
129. Hofmann M, Wollert KC, Meyer GP, Menke A, Arseniev L, Hertenstein B, et al. Monitoring of bone marrow cell homing into the infarcted human myocardium. *Circulation* 2005; **111**: 2198–202. doi: 10.1161/01.CIR.0000163546.27639.AA
130. Hou D, Youssef EA, Brinton TJ, Zhang P, Rogers P, Price ET, et al. Radiolabeled cell distribution after intramyocardial, intracoronary, and interstitial retrograde coronary venous delivery: implications for current clinical trials. *Circulation* 2005; **112** (Suppl 9): I150–6.
131. Nguyen PK, Lan F, Wang Y, Wu JC. Imaging: guiding the clinical translation of cardiac stem cell therapy. *Circ Res* 2011; **109**: 962–79. doi: 10.1161/CIRCRESAHA.111.242909
132. Gorelik M, Orukari I, Wang J, Galpoththawela S, Kim H, Levy M, et al. Use of MR cell tracking to evaluate targeting of glial precursor cells to inflammatory tissue by exploiting the very late antigen-4 docking receptor. *Radiology* 2012; **265**: 175–85. doi: 10.1148/radiol.12112212
133. Reisman M, Adams KT. Stem cell therapy: a look at current research, regulations, and remaining hurdles. *P T* 2014; **39**: 846–57.
134. van der Bogt KE, Schrepfer S, Yu J, Sheikh AY, Hoyt G, Govaert JA, et al. Comparison of transplantation of adipose tissue- and bone marrow-derived mesenchymal stem cells in the infarcted heart. *Transplantation* 2009; **87**: 642–52. doi: 10.1097/TP.0b013e31819609d9
135. van der Bogt KE, Sheikh AY, Schrepfer S, Hoyt G, Cao F, Ransohoff KJ, et al. Comparison of different adult stem cell types for treatment of myocardial ischemia. *Circulation* 2008; **118**(Suppl 14): S121–9. doi: 10.1161/CIRCULATIONAHA.107.759480
136. Janowski M, Engels C, Gorelik M, Lyczek A, Bernard S, Bulte JW, et al. Survival of neural progenitors allografted into the CNS of immunocompetent recipients is highly dependent on transplantation site. *Cell Transpl* 2014; **23**: 253–62. doi: 10.3727/096368912X661328
137. van Buul GM, Siebelt M, Leijs MJ, Bos PK, Waarsing JH, Kops N, et al. Mesenchymal stem cells reduce pain but not degenerative changes in a mono-iodoacetate rat model of osteoarthritis. *J Orthop Res* 2014; **32**: 1167–74. doi: 10.1002/jor.22650
138. Fan W, Cheng K, Qin X, Narsinh KH, Wang S, Hu S, et al. mTORC1 and mTORC2 play different roles in the functional survival of transplanted adipose-derived stromal cells in hind limb ischemic mice *via* regulating inflammation *in vivo*. *Stem Cells* 2013; **31**: 203–14. doi: 10.1002/stem.1265
139. Liang Y, Walczak P, Bulte JW. The survival of engrafted neural stem cells within hyaluronic acid hydrogels. *Biomaterials* 2013; **34**: 5521–9. doi: 10.1016/j.biomaterials.2013.03.095
140. Hwang do W, Jin Y, Lee do H, Kim HY, Cho HN, Chung HJ, et al. *In vivo* bioluminescence imaging for prolonged survival of transplanted human neural stem cells using 3D biocompatible scaffold in corticectomized rat model. *PLoS One* 2014; **9**: e105129. doi: 10.1371/journal.pone.0105129
141. Thomas DC, Wong FS, Zaccone P, Green EA, Wållberg M. Protection of islet grafts through transforming growth factor-β-induced tolerogenic dendritic cells. *Diabetes* 2013; **62**: 3132–42. doi: 10.2337/db12-1740
142. Bulte JW. Science to practice: can stem cells be labeled inside the body instead of outside? *Radiology* 2013; **269**: 1–3. doi: 10.1148/radiol.13131753